Direct measurements of the constant-volume heat capacity of solid parahydrogen from 22.79 to 16.19 cm^3/mole and the resulting equation of state

J. K. Krause* and C. A. Swenson
Ames Laboratory-USDOE and Department of Physics, Iowa State University, Ames, Iowa 50011
(Received 24 September 1979)

The constant-volume heat capacity of solid parahydrogen (p-H_2) has been measured directly from below 4 K to the melting line for six molar volumes (22.787 to 16.19 cm^3/mole). These data have been analyzed using the Mie-Grüneisen equation of state (EOS) to give the volume and temperature dependence of the Grüneisen parameter and the EOS for p-H_2, as well as the volume dependence of the quadrupole-quadrupole interaction parameter for orthohydrogen impurities. Good agreement is found with earlier 4-K high-pressure compression data, and reasonable agreement with direct strain-gauge measurements of $P(V,T)$. The thermodynamic properties for solid p-H_2 at $P=0$ are obtained by extrapolation to larger molar volumes, with the $T=0$, $P=0$ equilibrium volume given as 23.234 ($\pm$0.05) cm^3/mole and the triple-point volume of the solid as 23.48 ($\pm$0.05) cm^3/mole. The rather large temperature dependence of the Grüneisen parameter which results from a comparison with high-pressure melting-line data is discussed in terms of an explicit temperature dependence of the lattice vibration spectrum. No indications were found for phase transitions in solid p-H_2, nor for premelting anomalies.

I. INTRODUCTION

A study of the thermodynamic properties of solidified parahydrogen (p-H_2, nuclear spin $I=0$, rotational quantum number $J=0,2,\ldots$) has at least two direct applications. First, volume-dependent thermodynamic data for this elementary solid can provide a test of intermolecular potentials and also of methods for calculating extremely anharmonic lattice properties. Existing thermodynamic data for p-H_2 are quite uncertain, with conflicting evidence for even the $T=0$, $P=0$ molar volume, V_0.[1-3] A second application provides tests of semiempirical, phenomenological models for the lattice properties of solids. Solid hydrogen is extremely compressible, with a reduction in volume of approximately 30% (to 0.7 V_0) occurring at a $T=0$ pressure of 2000 bar. Hence, large changes in thermodynamic properties should be produced by modest pressures, more so than for any other solid except helium.

Our volume- and temperature-dependent measurements[4] of the heat capacity at constant volume $[C_V(T,V)]$ for solid p-H_2 are very similar to those carried out on the same solid by Ahlers.[5] The apparatus is that used by Fugate and Swenson[6] for measurements on solid neon. The differences from Ahlers's experiment are more in detail than substance, with higher accuracy and extended pressure and temperature ranges. Data for the present 6 molar volumes extend from 1 K to the melting line, with melting pressures which range from 60 bar at 15.6 K to 2400 bar at 52 K, and with corresponding $T=0$ pressures from 36 to 2100 bar. The $T=0$ equation of state (EOS) which is derived from these data can be used to test the low-pressure extrapolated region of the 4-K, 24-kbar isotherm of Anderson and Swenson.[3] Additional comparisons can be made with a direct EOS determination[1,2] for which a strain gauge was used to measure pressure changes in a bomb over roughly the same temperature and pressure range as for the present experiments.

Pure p-H_2 samples cannot be prepared in practice, since a residual orthohydrogen (o-H_2, $I=1$, $J=1,3,\ldots$) contribution always is present. This "impurity" affects the data in two ways. First, a quadrupole interaction between o-H_2 pairs splits the rotational degeneracy and produces a low-temperature heat capacity anomaly.[7] Second, the spin-spin interaction between o-H_2 pairs results in a spontaneous transformation of o-H_2 molecules into p-H_2 molecules, with the large energy difference ($\epsilon/k_B = 171$ K)[8] generating considerable heat. The first of these effects masks the low-temperature (Debye) portion of the lattice heat capacity, while the second makes calorimetry difficult due to background heating. We previously have reported[8] the existence of an anomalous enhanced ortho-para conversion which occurs at high temperatures (20 to 30 K) for small molar volumes, and which allows in one week the reduction of initial 5% o-H_2 concentrations to below 1%. The correction of the present results for the residual o-H_2 concentrations was straightforward and introduced only small ambiguities in the final results.

Sections II–V first describe the experiment and the data analysis and then the final results for C_V and thermodynamic properties derived from it. The Mie-Grüneisen EOS is used as a first ap-

proximation to derive an EOS for pure p-H_2 which is based on thermodynamic parameters along the melting line (P_m, T_m, V_m). This EOS, which gives extrapolated molar volumes and other thermodynamic properties at $P = 0$, then is compared with other results. Finally, the EOS is extended to much higher temperatures and pressures (18.7 kbar and 164 K) using the melting line results of Liebenberg *et al.*[9] in conjunction with the low-temperature results of Anderson and Swenson.[3]

II. EXPERIMENTAL PROCEDURES AND RESULTS

A. Experimental details

The apparatus and procedures which were used[4] were identical to those used by Fugate and Swenson[6] for similar experiments with solid neon. Very briefly, the calorimeter consisted of a 2.9-cm^3 beryllium copper bomb which was connected to room temperature by a narrow, vacuum-jacketed capillary. A heater was used to keep the capillary above the freezing temperature when the bomb was being filled along the melting line. Once the bomb was filled, the capillary was allowed to cool to 4 K and was blocked by solid. No slippage was observed, with the melting points on initial freezing and on final warming always the same. A calibrated germanium resistance thermometer and heaters on the bomb were used to obtain heat capacity data by means of the standard heat-pulse technique. The quantity of gas in the bomb was determined to better than 0.1% at room temperature after the experiment by measuring the pressure in a calibrated thermostated glass bulb into which the sample was released as the bomb was warmed. The molar volumes and number of moles for each of our six samples are given in cols. 2 and 3 of Table I.

The oil-gas separator used previously to compress neon[6] was modified by the manufacturers, Autoclave Engineers, for use with hydrogen by the insertion of a 286 stainless steel linear to prevent embrittlement. A silicone fluid (Dow Corning 200) was used in place of oil. The original 20 K equilibrium H_2, which was prepared by catalysis in the liquid (0.2% o-H_2), suffered considerable back-conversion towards 300 K equilibrium H_2 (75% o-H_2) in the separator under pressure. This was shown by direct measurement and by the magnitudes of the pairs anomaly (see below) and the spontaneous conversion heating rate in the samples. The o-H_2 concentrations in the samples were reduced by two procedures. First, following Ahlers,[10] the bomb was filled at low pressure (approximately 0.125 mole) directly from glass bulbs which were filled with freshly prepared p-H_2 and then was pressurized with gas from the separator to obtain the smaller molar volumes. This procedure resulted in an average o-H_2 concentration which was considerably below that which would have been obtained if all of the gas had been compressed in the separator. Second, the three highest pressure samples were each held for a week or so at temperatures where the enhanced

TABLE I. Physical properties of hydrogen at the equilibrium molar volume and for the six samples.

Sample	V[a] (cm^3/mole)	n (mole)	Ortho concentration[b] (%)	T_m[a] (K)	P_m[a,c] (bar)	P_0 (bar)	Θ_0[d] (K)	Θ_0[e] (K)	γ_0	B_0 (bar)
	23.234			14.42	18.85	0		120.64	2.344	1 759
H_2-1	22.221	0.130 67	3.0; 1.4	17.377	121.2	91.9	134.9	133.7	2.267	2 366
	(22.229)			(17.352)	(120.2)					
H_2-2	22.787	0.127 38	1.1; 0.32	15.667	59.6	36.5	126.6	126.3	2.309	2 008
	(22.795)			(15.644)	(58.9)					
H_2-3	19.120	0.152 48	0.7; 2.2	30.357	761.3	666.5	185.0	184.7	2.037	5 588
	(19.132)			(30.291)	(757.4)					
H_2-4	20.685[f]	0.140 58	<0.5; 0.14	22.822	355.1	302.2	156.3	156.0	2.153	3 641
	(20.698)			(22.768)	(352.5)					
H_2-5	17.458	0.167 69	<0.5; 0.25	40.944	1477	1306	220.8	221.16	1.913	8 808
	(17.476)			(40.811)	(1467)					
H_2-6	16.193	0.181 76	8.8; 0.07	51.776	2374	2104	253.2	254.7	1.819	12 540
	(16.219)			(51.534)	(2352)					

[a] Values in parentheses indicate measurements along the melting line before the correction to $V(T = 0)$.
[b] Directly measured; estimated from C_{pair}.
[c] Values are determined from the melting relation of Goodwin (Ref. 11).
[d] Calculated from fit to pairs anomaly.
[e] Calculated using the reduced relation.
[f] Possibly should be 20.705. See text.

anomalous conversion rate was a maximum.[4,8]

The first entry in col. 4 of Table I gives the results of direct room-temperature thermal conductivity cell measurements of the o-H_2 concentration in the gas after the experiment, while the second entry is an effective value which is derived from the magnitude of the pairs heat capacity anomaly (see below). The higher room-temperature values may be due to the inclusion of all o-H_2 molecules (not only pairs) and/or to back-conversion which was catalyzed by the bomb walls near the melting line as the sample was released at the end of the experiment. This certainly is the case for H_2-6, but the lack of consistency is puzzling. For our purposes, the "pairs" value has the greater significance since it is characteristic of the low-temperature anomaly.

B. Data and analysis

A complete discussion of the analysis and a tabulation of the data points are given elsewhere,[4] with only a brief summary given below. The accuracy of the data for both the addenda (unfilled bomb) and the sample was estimated to be 0.1%. The sample heat capacity varied from approximately 70% of the measured heat capacity for the largest molar volume to between 25% (below 5 K) and 50% (above 15 K) for the smallest molar volume.[4] The sample heat capacities were corrected in two ways to obtain C_V at constant volume. The first correction (maximum 1.4% at 50 K) compensated for the pressure increase inside the bomb and consequent sample expansion during a heat pulse and is required to obtain C_V from the measured sample heat capacity. The second correction (maximum 0.5% at 50 K) reduces these C_V values to true constant-volume conditions, since the result of the first correction is $C_V(V(T), T)$. Molar volumes (Table I, column 2) were calculated from the quantity of sample and the low-temperature bomb volume at the actual sample pressure. Columns 5 and 6 of Table I give the measured melting temperatures (T_m) and the calculated melting pressures for these temperatures (P_m),[11] while column 7 gives the $T = 0$ bomb pressure (P_0) as calculated from these experiments for each sample. The highest melting pressure was measured directly in terms of the pressure gauge on our system,[12] and coincides with an extrapolation of the expression given by Goodwin.[11] The quantities in parentheses are those obtained along the melting line before correction to constant ($T = 0$) volume.

Figure 1, which gives low-temperature experimental results for three characteristic samples, shows the effects of the o-H_2 pairs anomaly. The two runs for 19.120 cm^3/mole (H_2-3) show a six-

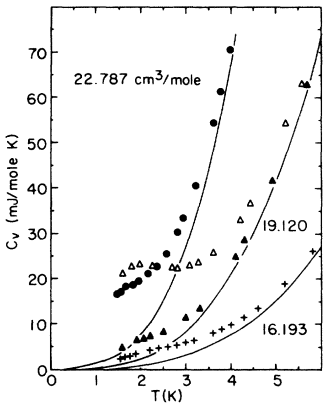

FIG. 1. Low temperature heat capacity data showing the effects of o-H_2 impurities. Data at 19.12 cm^3/mole are for two different o-H_2 concentrations. The solid lines represent lattice contribution.

fold reduction in the magnitude of the pairs heat capacity after the sample had been held in the accelerated conversion[8] region near 13 K for three days. Even for small o-H_2 concentrations such as those for the 22.787 (H_2-2) and 16.193 (H_2-6) cm^3/mole samples, the pairs anomaly is significant and a correction must be applied to obtain the lattice heat capacity for p-H_2. The form of this correction is not obvious, since time-, temperature-, and volume-dependent effects occur in the o-H_2 impurity system.[7,13] Spin diffusion causes o-H_2 molecules to cluster as the temperature is lowered, with the clustering breaking up as the temperature is increased, with the rates depending on temperature, volume, and concentration.[7,14] At sufficiently low temperatures, the o-H_2 pairs distribution remains fixed (long time constant), and a heat capacity contribution based on a fixed-pairs distribution model should apply.[7] A second possibility at higher temperatures is that an equilibrium distribution of o-H_2 pairs is achieved at all times, leading to a quite different form of heat capacity contribution.[7] Our low-temperature results can be fit very well by the fixed pairs model,[4] and this has been used in the analysis given below.

These low-temperature pairs anomalies are characterized by the molecular quadrupole-quadrupole coupling parameter, Γ, which presumably varies as $V^{-5/3}$,[7] with $\Gamma/k_B = 0.9\ (\pm 0.1)$ K at low temperature and zero pressure.[7] An explicit expression can be written[7] in the fixed pairs model for $C_{\text{pair}}(x)$, with $x = \Gamma/k_B T$ and a high-temperature limit which is given by

$$C_{\text{pair}} = k_B(Ax^2 + Bx^3) \quad (x \ll 1). \tag{1}$$

We have calculated $C_{\text{pair}}(x)$ at 26 points for $0.2 < x < 0.7$ and have found that Eq. (1) fits these calcu-

lations to better than 1% with

$$C_{\text{pair}} = k_B(7.901x^2 - 8.399x^3) \quad (x < 0.7). \tag{2}$$

This is strictly an empirical result and does not correspond to the high-temperature limit of the exact fixed pairs relation.

Hence, the results in Fig. 1 should correspond to a relationship of the form

$$C_V = C_{\text{an}} + C_{\text{latt}} = A'T^{-2} + B'T^{-3} + A_3T^3 + A_5T^5 + \cdots, \tag{3}$$

where $C_{\text{an}} = N_{\text{pair}}C_{\text{pair}}$, and the terms containing $A_3 (= 233.8nR\Theta_0^{-3})$ and A_5 represent the Debye and next higher contributions to the lattice heat capacity. As Ahlers[5] suggested, we have rewritten Eq. (3) in the form

$$(C_V - A_3T^3 - A_5T^5)T^2 = A' + B'/T, \tag{4}$$

and for an assumed value of A_5 (derived from high-temperature results where the pairs contribution is small), have adjusted A_3 to give the best fit of the relation to the data for each of our samples. Figures 2 and 3 give plots of Eq. (4) for the two different H_2-3 (19.120 cm^3/mole) o-H_2 concentrations shown in Fig. 1. The fit is excellent for these two concentrations for $T^{-1} > 0.3$ K^{-1}, and similar fits were obtained for the other samples. The values of Θ_0 which correspond to the best-fit A_3's are given in Table I, column 8, where they can be compared with those in column 9 which were obtained from the lattice heat capacity (see below).

The deviations for $T^{-1} < 0.3$ K^{-1} in Fig. 3 are characteristic of those we find in other samples (H_2-4, H_2-6) and are believed to be due to clustering effects.[7] The sample initially is quenched from 4 to approximately 1.5 K, with the pairs distribution characteristic of 4 K frozen in. As data are taken and the sample is warmed, clustering occurs towards an equilibrium low-temperature

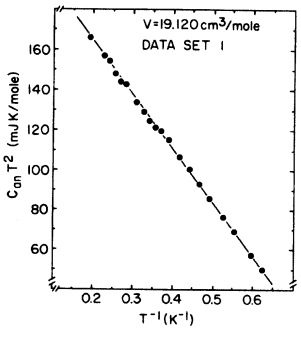

FIG. 2. Determination of the pairs contribution to the heat capacity for a sample with relatively large (2.2%) o-H_2 concentration [see Eq. (4)]. The straight line represents the two-term approximation [Eq. (2)]. This analysis was used to determine the lattice heat capacity (Tables I, IV).

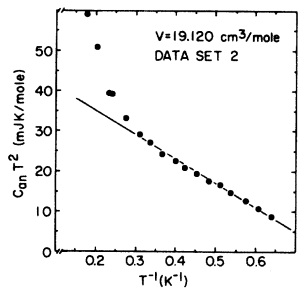

FIG. 3. A plot similar to that of Fig. 2 for data taken after the same sample had been held in the anomalous conversion region for several days to reduce the o-H_2 pairs concentration. The deviations for $T^{-1} < 0.3$ K^{-1} are believed to be due to clustering effects, as is discussed in the text.

distribution with an increase in the number of o-H_2 pairs and a consequent increase in the anomalous heat capacity over that which is extrapolated from the low-temperature region. The time constant increases with o-H_2 concentration,[14] so these effects were observed primarily for low o-H_2 samples. This time-dependent heat capacity was investigated specifically in measurements where the heat capacity was determined as a function of time at several average temperatures.[4] The time constants observed in these experiments varied from 1.5 to 5.5 h.

A comparison of Eqs. (2) and (4) shows that their ratio will give a determination of the effective number of o-H_2 pairs, and the second set of o-H_2 concentrations in Table I, column 4, was calculated from the anomaly fits. The ratio B'/A' is proportional to Γ, with Fig. 4 showing the volume dependence of the values of Γ obtained in this manner together with an extrapolation from the

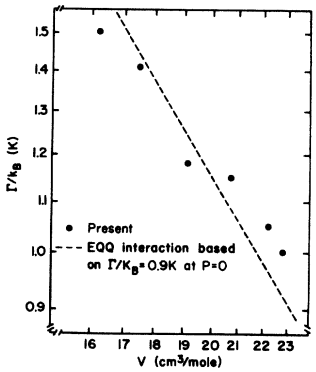

FIG. 4. A plot of the electric quadrupole-quadrupole EQQ coupling constant as a function of volume as derived from the observed anomalies and the two-term approximation. The dashed line represents an extrapolation to smaller molar volumes[7] of $P = 0$ results with the assumption of a $V^{-5/3}$ volume dependence.

TABLE II. Thermodynamic functions for sample H_2-1 ($V = 22.221$ cm^3/mole).

T (K)	C_V (J/mole K)	U_{th} (J/mole)	S (J/mole K)	P (bar)	Θ (K)
0	0	0	0	91.90	134.53
1	8.029×10^{-4}	2.003×10^{-4}	2.670×10^{-4}	91.90	134.27
2	6.541×10^{-3}	3.244×10^{-3}	2.159×10^{-3}	91.90	133.46
3	2.279×10^{-2}	1.677×10^{-2}	7.425	91.92	132.06
4	5.656	5.464	1.809×10^{-2}	91.96	130.04
5	1.172×10^{-1}	1.388×10^{-1}	3.662	92.05	127.51
6	2.168	3.020	6.610	92.51	124.65
7	3.694	5.901	1.102×10^{-1}	92.51	121.75
8	5.890	1.063×10^{0}	1.730	93.00	119.07
9	8.864	1.794	2.588	93.74	116.79
10	1.266×10^{0}	2.864	3.711	94.81	114.97
11	1.727	4.354	5.128	96.36	113.58
12	2.264	6.343	6.856	98.40	112.50
13	2.873	8.906	8.904	101.02	111.59
14	3.552	1.211×10^{1}	1.128×10^{0}	104.31	110.67
15	4.296	1.603	1.398	108.33	109.71
16	5.088	2.072	1.700	113.15	108.76
17	5.954	2.623	2.034	118.82	107.48
17.38	6.347	2.855	2.169	121.21	106.51

low pressure result[7] ($\Gamma/k_B = 0.9$ K at 23.23 cm^3/mole) using the $V^{-5/3}$ volume dependence. The agreement shown in Fig. 4 together with the consistency between the Θ_0's derived from this analysis and those from fits to the lattice contribution (see below) lends credence to the validity of our analysis.

Clustering effects cause uncertainties in the magnitude of the pairs anomaly correction which must be applied to obtain the lattice contribution at "high" temperature. Clustering (indicated by deviations as in Fig. 3) was observed for samples H_2-3 (set 2), H_2-4, and H_2-6, but not for H_2-1, H_2-3 (set 1) nor H_2-5 (set 2). Here, the second set of data always has the lower o-H_2 concentrations (see Figs. 1–3). We have arbitrarily chosen to accept as correct the extrapolations to $T = 0$ of H_2-3 (set 1) and H_2-5 (set 2) (see below) and to view as suspect other data for which the anomalous contribution is greater than 5% of the lattice heat capacity.

Polynomials of the form

TABLE III. Thermodynamic functions for sample H_2-2 ($V = 22.787$ cm^3/mole).

T (K)	C_V (J/mole K)	U_{th} (J/mole)	S (J/mole K)	P (bar)	Θ (K)
0	0	0	0	36.50	126.49
1	9.667×10^{-4}	2.412×10^{-4}	3.214×10^{-4}	36.50	126.22
2	7.889×10^{-3}	3.910×10^{-3}	2.602×10^{-3}	36.50	125.38
3	2.755×10^{-2}	2.025×10^{-2}	8.962	36.52	123.96
4	6.856	6.610	2.187×10^{-2}	36.57	121.97
5	1.423×10^{-1}	1.682×10^{-1}	4.436	36.67	119.51
6	2.636	3.666	8.019	36.88	116.78
7	4.492	7.170	1.338×10^{-1}	37.24	114.04
8	7.164	1.292×10^{0}	2.103	37.82	111.52
9	1.076×10^{0}	2.181	3.145	38.72	109.38
10	1.531	3.477	4.506	40.04	107.68
11	2.076	5.273	6.214	41.86	106.40
12	2.701	7.656	8.283	44.29	105.41
13	3.408	1.070×10^{1}	1.072×10^{0}	47.38	104.47
14	4.204	1.450	1.353	51.25	103.24
15	5.049	1.913	1.672	55.97	102.32
15.67	5.513	2.266	1.902	59.58	102.69

TABLE IV. Thermodynamic functions for sample H_2-3, data set 1 ($V = 19.120$ cm^3/mole).

T (K)	C_V (J/mole K)	U_{th} (J/mole)	S (J/mole K)	P (bar)	Θ (K)
0	0	0	0	666.50	184.67
1	3.095×10^{-4}	7.730×10^{-5}	1.0305×10^{-4}	666.50	184.50
2	2.498×10^{-3}	1.244×10^{-3}	8.288	666.50	183.95
3	8.560	6.362	2.822×10^{-3}	666.51	183.03
4	2.074×10^{-2}	2.040×10^{-2}	6.777	666.52	181.71
5	4.167	5.074	1.346×10^{-2}	666.56	179.99
6	7.457	1.077×10^{-1}	2.376	666.62	177.90
7	1.234×10^{-1}	2.052	3.868	666.73	175.49
8	1.927	3.613	5.943	666.89	172.86
9	2.878	5.991	8.733	667.15	170.12
10	4.141	9.472	1.239×10^{-1}	667.52	167.42
11	5.767	1.440×10^{0}	1.707	668.05	164.88
12	7.792	2.114	2.292	668.78	162.62
13	1.023×10^{0}	3.012	3.010	669.74	160.71
14	1.308	4.174	3.870	670.99	159.20
16	1.990	7.446	6.044	674.50	157.13
18	2.820	1.224×10^{1}	8.855	679.63	155.48
20	3.765	1.880	1.231×10^{0}	686.69	154.46
22	4.794	2.735	1.637	695.89	153.53
24	5.887	3.802	2.101	707.42	152.55
26	7.034	5.094	2.617	721.43	151.29
28	8.224	6.619	3.182	738.09	149.62
30	9.450	8.385	3.790	757.56	147.44
30.36	9.677	8.727	3.904	761.35	146.95

$$C_V = \sum_{\text{odd } n>1} A_n T^n \qquad (5)$$

were fitted to the anomaly-corrected heat capacity data for various overlapping temperature ranges, generally with root-mean-square deviations of the data from the fit of approximately 0.2%. These polynomials then were used to generate the

TABLE V. Thermodynamic functions for sample H_2-4 ($V = 20.685$ cm^3/mole).

T (K)	C_V (J/mole K)	U_{th} (J/mole)	S (J/mole K)	P (bar)	Θ (K)
0	0	0	0	302.20	156.20
1	5.125×10^{-4}	1.279×10^{-4}	1.705×10^{-4}	302.20	155.95
2	4.159×10^{-3}	2.066×10^{-3}	1.376×10^{-3}	302.20	155.20
3	1.437×10^{-2}	1.063×10^{-2}	4.710	302.21	153.99
4	3.518	3.433	1.139×10^{-2}	302.24	152.35
5	7.150	8.615	2.280	302.29	150.34
6	1.294×10^{-1}	1.845×10^{-1}	4.058	302.40	148.03
7	2.173	3.551	6.670	302.58	145.30
8	3.432	6.318	1.035×10^{-1}	302.87	142.60
9	5.157	1.057×10^{0}	1.534	303.31	140.04
10	7.423	1.681	2.189	303.97	137.74
11	1.028×10^{0}	2.561	3.026	304.89	135.77
12	1.374	3.757	4.064	306.14	134.15
13	1.778	5.329	5.320	307.78	132.86
14	2.235	7.332	6.802	309.88	131.86
16	3.282	1.282×10^{1}	1.045×10^{0}	315.63	130.48
18	4.490	2.057	1.500	323.75	129.21
20	5.840	3.088	2.042	334.61	127.61
22	7.258	4.396	2.664	348.44	125.93
22.82	8.015	5.022	2.943	355.09	123.75

TABLE VI. Thermodynamic functions for sample H_2-5, data set 2 ($V = 17.458$ cm^3/mole).

T (K)	C_V (J/mole K)	U_{th} (J/mole)	S (J/mole K)	P (bar)	Θ (K)
0	0	0	0	1306.00	221.16
1	1.801×10^{-4}	4.499×10^{-5}	5.997×10^{-5}	1306.00	221.01
2	1.449×10^{-3}	7.227×10^{-4}	4.815×10^{-4}	1306.00	220.55
3	4.943	3.684×10^{-3}	1.635×10^{-3}	1306.00	219.79
4	1.189×10^{-2}	1.176×10^{-2}	3.911	1306.01	218.70
5	2.369	2.908	7.728	1306.03	217.28
6	4.194	6.128	1.355×10^{-2}	1306.07	215.53
8	1.057×10^{-1}	2.019×10^{-1}	3.334	1306.23	211.13
10	2.226	5.195	6.830	1306.58	205.91
12	4.165	1.144×10^{0}	1.247×10^{-1}	1307.28	200.52
14	7.105	2.252	2.096	1308.50	195.69
16	1.117×10^{0}	4.061	3.297	1310.50	191.99
18	1.632	6.794	4.900	1313.52	189.56
20	2.253	1.066×10^{1}	6.932	1317.80	187.85
22	2.967	1.587	9.407	1323.56	186.53
24	3.753	2.258	1.232×10^{0}	1330.99	185.59
26	4.588	3.091	1.565	1340.24	184.93
28	5.456	4.095	1.937	1351.41	184.42
30	6.348	5.275	2.344	1364.59	183.86
32	7.265	6.636	2.782	1379.85	183.07
34	8.206	8.183	3.251	1397.31	181.91
36	9.163	9.920	3.747	1417.07	180.39
38	1.012×10^{1}	1.185×10^{2}	4.268	1439.24	178.60
40	1.110	1.397	4.812	1463.96	176.15
40.94	1.162	1.504	5.077	1476.61	174.20

TABLE VII. Thermodynamic function for sample H_2-6 ($V = 16.193$ cm^3/mole).

T (K)	C_V (J/mole K)	U_{th} (J/mole)	S (J/mole K)	P (bar)	Θ (K)
0	0	0	0	2104.00	254.22
2	9.531×10^{-4}	4.754×10^{-4}	3.168×10^{-4}	2104.00	253.63
4	7.784×10^{-3}	7.713×10^{-3}	2.566×10^{-3}	2104.01	251.88
6	2.717×10^{-2}	3.995×10^{-2}	8.841	2104.05	249.08
8	6.738	1.302×10^{-1}	2.155×10^{-2}	2104.15	245.35
10	1.389×10^{-1}	3.302	4.357	2104.38	241.00
12	2.563	7.163	7.845	2104.82	235.78
14	4.358	1.397×10^{0}	1.305×10^{-1}	2105.60	230.43
16	6.913	2.510	2.045	2106.87	225.71
18	1.030×10^{0}	4.217	3.046	2108.81	222.03
20	1.450	6.684	4.342	2111.61	219.45
22	1.948	1.007×10^{1}	5.952	2115.45	217.71
24	2.517	1.452	7.886	2120.51	216.45
26	3.144	2.018	1.014×10^{0}	2126.94	215.59
28	3.833	2.714	1.272	2134.87	214.68
30	4.564	3.554	1.562	2144.44	213.86
32	5.323	4.542	1.880	2155.74	213.14
34	6.099	5.684	2.226	2168.83	212.49
36	6.882	6.982	2.597	2183.76	211.85
38	7.669	8.437	2.990	2200.58	211.15
40	8.458	1.005×10^{2}	3.404	2219.34	210.31
42	9.247	1.182	3.835	2240.10	209.26
44	1.003×10^{1}	1.375	4.284	2262.94	207.98
46	1.081	1.583	4.747	2287.95	206.52
48	1.157	1.807	5.223	2315.25	204.92
50	1.233	2.046	5.711	2345.01	202.90
51.78	1.308	2.272	6.154	2373.78	199.82

smoothed lattice heat capacity results which are given in Tables II–VII. Calculated values for the internal energy U and the entropy S,

$$U = \int_0^T C_V dT, \quad S = \int_0^T C_V d\ln T, \tag{6}$$

are given also in these tables, together with the equivalent value of the Debye temperature Θ which corresponds to each $C_V(T)$. The solid line in each table indicates the temperature below which the observed pairs anomaly contribution was greater than 5% of the lattice heat capacity.

A useful correlation for these results is obtained through reduced plots $C_V(T/\Theta_0(V))$ or, more sensitively and equivalently, through plots of $\Theta/\Theta_0(V)$ vs $T/\Theta_0(V)$ which show deviations from Debye behavior. The representations which resulted from the use of Tables II–VII revealed in-consistencies in the volume dependence of Θ/Θ_0 at constant T/Θ_0 which appeared to result from incorrect extrapolations to $T = 0$. The reduced relations for H_2-3 (set 1) and H_2-5, for which clustering effects were small, were in agreement for $T/\Theta_0 < 0.06$ and were very similar to that for H_2-2. Hence, we assumed the reduced relation for these samples which appears in Table VIII, and then used it to determine Θ_0 and a new extrapolation for the other four samples. The resulting family of Θ/Θ_0 vs T/Θ_0 relations is shown in Fig. 5, with the corresponding values of $\Theta_0(V)$ given in Table I, column 9. The only serious (greater than 0.2%) discrepancy between these values of Θ_0 and those given in Tables II–VII occurs for the first sample which was run, H_2-1, and for which the pairs anomaly determination of Θ_0 also appears to be inconsistent with the reduced relation. This first sample also had the highest o-H_2 concentration. In every other case, agreement to better than 0.2% is found between the values of Θ_0 as determined by the reduced relation and fits to the pairs anomaly.

Figure 6 is a plot of $\ln\Theta_0$ vs $\ln V$ for the results in Table I, columns 2 and 9. The solid curve on this plot corresponds to the relation

$$\ln\Theta_0 = 8.4528 - 0.614\ \ln V - 0.0744V, \tag{7}$$

TABLE VIII. Reduced Θ/Θ_0 vs T/Θ_0 relation for low temperature.

T/Θ_0	Θ/Θ_0
0	1
0.01	0.9955
0.02	0.9850
0.03	0.9675
0.04	0.9440
0.05	0.9170
0.06	0.8920

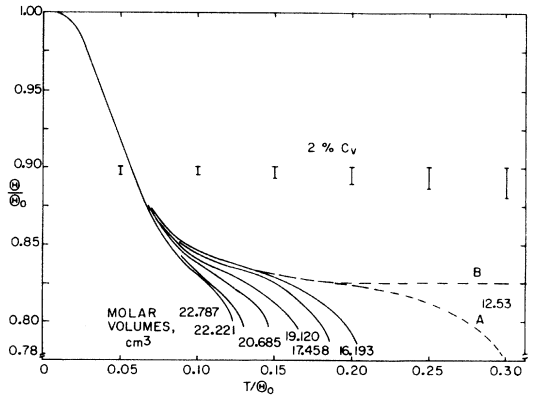

FIG. 5. Reduced heat capacity results. Curves A and B represent possible extrapolations to smaller molar volumes. See the text for details.

from which the limiting $T = 0$ Grüneisen parameter can be calculated as

$$\gamma = \frac{-d\ln\Theta_0}{d\ln V} = 0.614 + 0.0744V, \tag{8}$$

which is similar to that found for helium.[15] These relations are slightly different from those given originally.[4] The scatter of the Θ_0's about Eq. (7) corresponds to appreciably less than 0.1% in V and suggests at least an excellent internal consistency in the volume determinations. The exception is for sample H_2-4, for which the volume determination appears to be approximately 0.1% too low (i.e., should be 20.705 instead of 20.685 cm³/mole). Similar deviations of this magnitude and sign appear for this molar volume in the smooth $T = 0$ pressure-volume relation and in the temperature dependence of the volume of the solid along the melting curve. These results will be discussed in Sec. III.

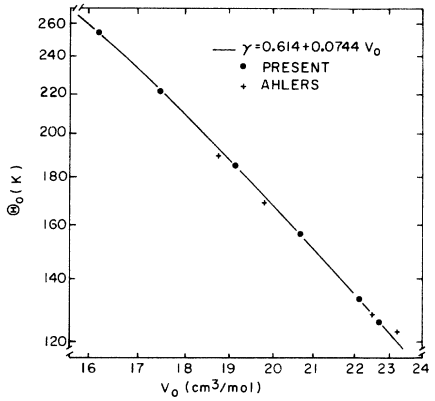

FIG. 6. The volume dependence of the limiting Debye temperature. The solid line represents a fit to the results which corresponds to the expression for the Grüneisen parameter [Eqs. (7) and (8)].

Figure 6 also contains Ahlers's determination of Θ_0 for three constant-volume measurements and for his $P=0$ constant pressure data.[5] The agreement is satisfactory, except perhaps at $P=0$. The shapes of his reduced relations are appreciably different from those in Fig. 5, however. In particular, if his data are fit to our reduced relation for temperatures above 8 K, his measured values of C_V are larger than ours by several percent at 4 K. His data were taken before clustering effects were recognized, and the excess heat capacity could be similar to that shown in our Fig. 3. A comparison of his $P=0$ heat capacities with those calculated from the present data will be given in Sec. III B below.

III. EQUATION OF STATE

A. $P(V,T)$

The present results $[C_V(T,V),\ V_m(T),\ P_m(T)]$ are sufficient to be able to calculate the equation of state for p-H_2:

$$P(V,T)=P(V,T_m)+\int_{T_m}^{T}\left(\frac{\partial S}{\partial V}\right)_T dT \tag{9}$$

using the Maxwell relation, $(\partial P/\partial T)_V=(\partial S/\partial V)_T$. This EOS can be compared with previous 4 K results from this laboratory[3] and with recent direct strain gauge measurements.[1,2] The $P=0$ thermodynamic properties, including the equilibrium molar volume $[V_0=V(T=0,P=0)]$, follow from this EOS by extrapolation.

The calculation of an EOS from our data is simplified considerably if the Mie-Grüneisen model is assumed to be approximately valid. The basic assumption of this model is that the volume dependence of the thermodynamic functions can be represented in terms of a characteristic temperature, $\Theta_0(V)$, where Θ_0 is the $T=0$ Debye temperature. Hence, the heat capacity at constant volume and the entropy can be written, respectively, as $C_V(T/\Theta_0(V))$ and $S(T/\Theta_0(V))$. Figure 5 shows that a relationship of this form exists for p-H_2 for $T/\Theta_0<0.06$. The Grüneisen relationship follows from this model as

$$\left(\frac{\partial P}{\partial T}\right)_V=\gamma_0(V)\frac{C_V}{V}=\left(\frac{\partial S}{\partial V}\right)_T, \tag{10}$$

where $\gamma_0=-d\ln\Theta_0/d\ln V$ is the Grüneisen parameter.

The next approximation is given by expressing the entropy and the heat capacity as explicit functions of V as well as of T/Θ_0 $[S(T/\Theta_0,V),\ C_V(T/\Theta_0,V)]$, so that

$$\left(\frac{\partial P}{\partial T}\right)_V=\left(\frac{\partial S}{\partial V}\right)_T=\gamma_0\frac{C_V}{V}+\left(\frac{\partial S}{\partial V}\right)_{T/\Theta_0}. \tag{11}$$

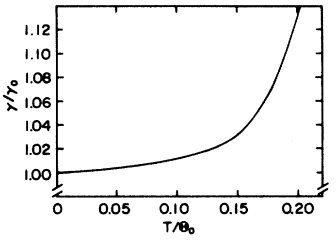

FIG. 7. The temperature dependence of the Grüneisen parameter.

Equation (10) then can be generalized to

$$\left(\frac{\partial P}{\partial T}\right)_V=\left(\frac{\partial S}{\partial V}\right)_T=\gamma(T,V)\frac{C_V}{V}, \tag{12}$$

with

$$\gamma(T,V)=\gamma_0(V)+\frac{V}{C_V(T,V)}\left(\frac{\partial S}{\partial V}\right)_{T/\Theta_0}. \tag{13}$$

The entropies in Tables II–VII give $(\partial S/\partial V)_{T/\Theta_0}$, while γ_0 is given by Eq. (8). The resulting temperature dependence of the ratio $\gamma(V,T)/\gamma_0$ scales with T/Θ_0 as is shown in Fig. 7. Hence, Eq. (9) can be evaluated as

$$P(V,T)=P_m(V,T_m)+\int_{T_m}^{T}\gamma(V,T)\frac{C_V}{V}dT. \tag{14}$$

This relation was used to calculate the temperature-dependent pressures which are given in Tables II–VII and which are plotted in Fig. 8.

The low-temperature pressure-volume relation, $P_0(V)$, was expressed in terms of the generalized Birch relation,[3]

$$P_0(V)=y^5(y^2-1)[A_1+A_2(y^2-1)], \tag{15}$$

with $y^3=V_0/V$, $V_0=23.234$ cm^3/mole, $A_1=2638.83$ bar, and $A_2=5869.50$ bar. The deviations of the low-temperature data (columns 2 and 7, Table I) from this relation were less than 0.1%. Equation

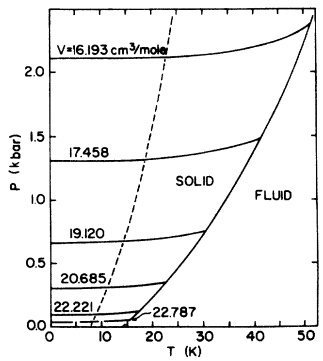

FIG. 8. Experimental isochores for solid p-H_2.[8] The dashed curve indicates the region of rapid ortho-to-para conversion.

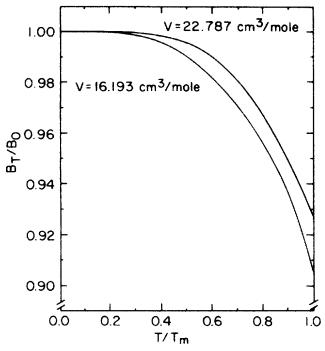

FIG. 9. The temperature dependence of the isothermal bulk modulus, with $B_0 = 2008$ bar at 22.787 cm^3/mole and 12 540 bar at 16.193 cm^3/mole.

(15) was differentiated to calculate the low-temperature bulk moduli, $B_0 = -dP_0/d\ln V$, which are given in Table I, column 11.

The temperature dependence at constant volume of the isothermal bulk modulus, $B_T = -(\partial P/\partial \ln V)_T$, can be calculated either by fits of Eq. (15) to the EOS or by a thermodynamic analysis of the data in Tables II–VII. The results of such an analysis[4] are given in Fig. 9 in terms of an arbitrary scaling with the melting temperature. These effects are quite large, but become smaller with decreasing molar volume. The accuracy of the B_T/B_0 relation perhaps is one percent or so, since the rather inexact calculation gives $1 - B_T/B_0$.

B. Thermodynamic properties at $P = 0$

The volume-dependent heat capacity results as given by Fig. 5 and Eq. (7), the volume- and temperature-dependent bulk moduli and Grüneisen parameters and, initially, an estimated $V(T, P = 0)$ relation were used with the Grüneisen relation [Eq. (12)] to calculate self-consistently the $P = 0$ volume thermal expansion coefficient,

$$\beta(T, P = 0) = \left(\frac{\partial \ln V}{\partial T}\right)_p = \frac{\gamma C_V}{B_T V} \tag{16}$$

[since $\beta B_T = (\partial P/\partial T)_V$] as well as the heat capacity at constant pressure C_P. The results of these calculations are given in Table IX. Only a few comparisons are possible with other results, with the absolute values of the molar volumes to be discussed in Sec. IV. Our value for Θ_0(120.64 K) is somewhat lower than that given by direct low-temperature measurements [122 K (Ref. 7), 124.5 ± 1 K (Ref. 16)], although it is higher than that from neutron scattering measurements (118 K).[17] Ahlers[5] has measured C_P directly, with results which are lower than ours below 8 K (Θ_0 ~123 K), and which become larger by about 4% above 8 K. These differences are opposite to those which we find from the comparison of his constant volume measurements with ours, and hence are rather puzzling.

Thomas *et al.*[18] have used Brillouin scattering to determine the elastic constants of p-H_2 at saturated vapor pressure and 13.2 K. They calculate their results for a molar volume of 23.20 cm^3, while the present results suggest that the molar volume at 13.2 K should be 23.43 cm^3. Hence, the adiabatic bulk modulus which they give should be decreased from 1730 (±40) bar to 1713 (±40) bar. The present calculation gives $B_T = 1560$ bar at 13.2 K, which corresponds to $B_S = (C_p/C_V)B_T = 1701$ bar, with an uncertainty of 1% or so. The agreement is excellent.

TABLE IX. $P = 0$ thermodynamic properties of parahydrogen.

T (K)	V (cm^3/mole)	C_V [a] (J/mole K)	C_P (J/mole K)	γ	β (K^{-1})	B_T (bar)
0	23.234	0	0	2.344	0	1759
1	23.234	1.11×10^{-3}	1.11×10^{-3}	2.344	6.4×10^{-7}	1759
2	23.234	9.22	9.22	2.344	5.3×10^{-6}	1759
3	23.234	3.22×10^{-2}	3.22×10^{-2}	2.344	1.85×10^{-5}	1759
4	23.235	7.98	7.98	2.344	4.58	1758
5	23.237	1.668×10^{-1}	1.670×10^{-1}	2.345	9.59	1755
6	23.240	3.11	3.12	2.350	1.80×10^{-4}	1751
7	23.245	5.29	5.32	2.352	3.07	1744
8	23.255	8.54	8.62	2.356	4.99	1735
9	23.269	1.280×10^{0}	1.301×10^{0}	2.363	7.58	1715
10	23.290	1.818	1.865	2.368	1.092×10^{-3}	1693
11	23.320	2.470	2.567	2.372	1.51	1659
12	23.361	3.234	3.421	2.376	2.03	1618
13	23.415	4.135	4.48	2.389	2.69	1571
13.80	23.471	4.935	5.48	2.400	3.31	1525

[a] Corresponds to $\Theta_0 = 120.64$ K.

IV. DISCUSSION

Section III contains comparisons of the heat capacity data with other results, as well as a comparison of our extrapolated bulk modulus at 13.2 K with that derived from Brillouin scattering. The present discussion will concentrate on a comparison of our EOS with previous measurements and theoretical calculations and will include an analysis of the consistency of molar volume data. Recent determinations of the molar volumes of solid p-H_2 along the melting line to approximately 160 K make it possible to estimate the temperature dependence of the Grüneisen parameter along the melting line. The possibility that phase transitions exist in solid hydrogen also will be discussed.

A. Equation of state

Anderson and Swenson[3] (AS) have published 4-K isotherms for H_2 and D_2 which extend from roughly 500 bar to 24 kbar. Their results are expressed in terms of relative compressions, V/V_0, where the zero pressure reference compression ($V/V_0 = 1.000 \pm 0.002$ at $P = 0$) and bulk modulus [$B_0(V_0) = 1700 \mp 60$ bar] both were obtained by extrapolation to $P = 0$ from 500 bar. The AS results overlap the three highest pressure values of $P_0(V)$ in Table I and are consistent with them if an arbitrary $V_0 = 23.25$ cm^3/mole is used. The 0.07% difference between this effective value of V_0 and the present "true" value (23.234 cm^3/mole) is within the uncertainties quoted by AS. The present relation, which is valid from $P = 0$ to 2000 bars [Eq. (15) and the parameters following it], and the AS $P_0(V)$ relation (generated with $V_0 = 23.25$ cm^3/mole) are consistent between 500 bar and 2000 bar to within 1% in pressure and 1.5% in bulk modulus.

The AS experiments gave identical results for a single p-H_2 sample and for several samples for which the o-H_2 concentration was unknown, but was believed to be between 50% and 75%. Driessen *et al.*[2] show that the o-H_2 contribution to the 4-K isotherm for hydrogen becomes relatively small for pressures greater than 500 bar, and they comment that even if the AS samples contained 75% o-H_2, the extrapolation to $P = 0$ of the AS data could be characteristic of pure p-H_2 with no o-H_2 contribution. Hence, we have used a combination of the present results to 1500 bar for pure p-H_2 and the AS results from 1500 bar to 24 kbar (using $V_0 = 23.25$ cm^3/mole) to produce the 4-K isotherm for p-H_2 which is given in Table X.

Driessen *et al.*[2] have concluded from their constant-volume strain gauge measurements [$P(T, V = \text{constant})$] for solid hydrogen that the AS extrapolation to $P = 0$ is in error by considerably more than is suggested above, and they recommend a revised relation with $V_0 = 23.14$ (± 0.08) cm^3/mole and $B_0 = 1858$ bar. Their experiment gives sample pressure changes from $T = 0$ to the melting line which are greater than ours by from 20% at low pressure to 9% at their highest pressure. These differences are very close in magnitude to the quadrupole pressure corrections which they apply for their 50% o-H_2 samples, and also they are close to their estimated experimental uncertainties. The molar volumes which are used in their data analysis are based on an extrapolation upwards in pressure of an extrapolation to

TABLE X. $T = 0$ isotherm for p-H_2 as derived from the present results (above 17.0 cm^3/mole) and those of AS (17.0 cm^3/mole and smaller).

V (cm^3/mole)	P (kbar)	B_T (kbar)	V (cm^3/mole)	P (kbar)	B_T (kbar)
23.234	0	1.759	16.0	2.268	13.43
23.0	1.845×10^{-2}	1.886	15.5	2.727	15.52
22.5	6.311	2.18	15.0	3.28	17.96
22.0	1.159×10^{-1}	2.52	14.5	3.93	20.85
21.5	1.782	2.90	14.0	4.72	24.26
21.0	2.515	3.34	13.5	5.68	28.31
20.5	3.38	3.83	13.0	6.83	33.15
20.0	4.39	4.39	12.5	8.25	38.9
19.5	5.59	5.04	12.0	9.97	46.0
19.0	6.99	5.77	11.5	12.11	54.5
18.5	8.64	6.62	11.0	14.76	64.9
18.0	1.058×10^{0}	7.59	10.5	18.07	77.8
17.5	1.287	8.71	10.0	22.24	93.8
17.0	1.559	10.00	9.8	24.21	101.3
16.5	1.883	11.64			

$T = 0$ of the melting curve molar volumes of Younglove[19] (maximum $T = 0$ pressure, 300 bar). There is no overlap of the extrapolation to 4 K with the data of AS. Our direct determinations of the molar volumes along the melting line, together with the results of consistency checks with Younglove's and other data (see below), suggest that the present results and analysis are to be preferred over those given by Driessen *et al.*[2] Their tabulated empirical EOS is inconsistent with our results and also in the extrapolated region with recent higher temperature and pressure data (see below).[9]

Partial support for the Driessen *et al.*[2] reanalysis of the AS data is given by Silvera and Goldman[20] who use a semiempirical pair potential for H_2 and D_2 to calculate low temperature pressure-volume relations for these two solids. They find that for molar volumes near 10 cm^3 (approximately 20 kbar) their calculated common volume pressure differences for the two isotopes (2.0 to 2.5 kbar obtained using Driessen *et al.*'s[2] values for V_0) are larger than what they obtain from the AS results (1 kbar), with considerable improvement resulting when the Driessen *et al.*[2] modified relation for solid hydrogen is used. We find that the AS isotherm of Table X agrees well with their results at high pressure and gives a pressure difference between H_2 and D_2 at 10 cm^3/mole which is 1.84 kbar.

B. Molar volumes

The directly determined number of moles for each sample in Table I is believed to be accurate to ± 0.1%. The molar volumes have a somewhat greater potential systematic uncertainty since these require the bomb volume under pressure at low temperature. They are internally consistent [in terms of the smooth $T_m(V)$, $\Theta_0(V)$, and $P_0(V)$ relations], however, to appreciably better than 0.1%, with the exception of the molar volume for the H_2-4 sample. Hence, we believe that the low temperature equilibrium molar volume [$V_0(T = 0, P = 0)$, Sec. III A] is

$$V_0 = 23.234\ (\pm 0.05)\ \text{cm}^3/\text{mole}.$$

This is appreciably larger than the previously quoted values as summarized by Driessen *et al.*,[2] who prefer 23.14 (±0.08) cm^3/mole, although the error limits of the two values overlap. A reasonable overlap of all V_0 determinations would be given by $V_0 = 23.20$ (±0.05) cm^3/mole.[4,8]

The results for the temperature dependence of the molar volume of the solid along the melting line (Table I) can be represented to within 0.1% by a relation of the form suggested by Kechin *et al.*,[21]

$$V_m = a - b \ln T_m = 37.989 - 5.5269 \ln T_m . \qquad (17)$$

Previous results for $V_m(T)$ are given by Ahlers[5] for 16.35 K, and by Dwyer *et al.*[22] as reanalyzed by Younglove (see below).[19] Ahlers[5] gives 22.60 (±0.1) cm^3/mole, to be compared with 22.55 cm^3/mole as calculated from Eq. (17) for 16.35 K. Our three largest molar volumes overlap Younglove's results and are in agreement with them to within his stated uncertainties and ours, ±0.2%.[4]

Driessen *et al.*[2] suggest the empirical relationship that the thermal contribution to the pressure along the melting line $[P_{th}(T_m) + P_0(V) = P(V, T_m)]$ is a linear function of $P_0(V)$,

$$P_{th}(T_m(V)) = \alpha + \beta P_0(V), \qquad (18)$$

with the parameter α being the melting pressure for which the molar volume of the solid at melting is the equilibrium value V_0 [that is, $P_0(V_0) = 0$]. Data for our four largest molar volumes can be represented by such a relationship, with $\alpha = 18.85$ bar and $\beta = 0.1142$. Curvature is observed at smaller molar volumes. If Goodwin's melting relation[11] is used, $T_m = 14.42$ K and $V_0 = 23.240$ cm^3/mole from Eq. (17). Younglove,[19] however, gives melting pressures which are approximately 2% smaller than these near 14.4 K, so T_m becomes 14.43 K and $V_0 = 23.236$ cm^3/mole, in excellent agreement with the value given above.

Table IX gives the calculated molar volume at the triple point of p-H_2 (13.80 K) as $V_s^{tr} = 23.471$ cm^3, while the extrapolation of Eq. (17) to 13.80 K gives 23.483 cm^3/mole. The agreement is satisfactory since empirical extrapolations are involved for each determination. These values are quite different from those which appear in the literature. Dwyer *et al.*[22] used the Clausius-Clapeyron equation, their directly measured latent heats of fusion[23] and Goodwin's[11] melting-line relation $P_m(T)$ to calculate molar volume differences which are combined with Goodwin and Roder's[24] fluid molar volumes to obtain the molar volumes of the solid along the melting line. Their extrapolated result, $V_s^{tr} = 23.31$ cm^3/mole, is quoted by Roder *et al.*[25] in a compilation of properties of the hydrogen isotopes. As was stated above, Younglove[19] believes that the melting pressure relation of Goodwin[11] is incorrect below 16 K with a slope, dP_m/dT, which is too small by approximately 3% at the triple point. This suggests a triple point molar volume of 23.41 (±0.05) cm^3, although his relation[19] extrapolates to 23.38 cm^3/mole at 13.80 K. Grilly[26] has obtained $V_s^{tr} = 23.386$ (±0.05) cm^3/mole from a direct measurement of $V_L^{tr} - V_s^{tr} = 2.79$ cm^3/mole, and $V_L^{tr} = 26.176$ (±0.05) cm^3/mole as given by Goodwin and Roder.[24]

The internal consistency of the present results can be tested through the use of a thermodynamic relationship for the temperature dependence of

the molar volume along the melting line, where all quantities refer to the solid at melting,

$$\frac{dV_m}{dT} = \frac{V}{B_T}\left(\frac{\gamma C_V}{V} - \frac{dP_m}{dT}\right), \tag{19}$$

with dP_m/dT calculated from Goodwin's[11] expression, and the volume and temperature dependencies of the other quantities (C_V, γ, B_T) as given in this paper. The agreement between dV_m/dT as calculated from Eqs. (17) and (19) is better than 1% except for the smallest molar volume (the end of the range) where it is 2%. The temperature dependences of both γ and B_T are important for this calculation.

Equations (17) and (19) in addition can be combined to calculate $dP_m/dT = 31.0$ bars/K at the triple point, to be compared with that from Goodwin's[11] relation, 29.67 bar/K. The difference is 4.5% instead of the 3% stated by Younglove.[19] The value from the present data (31.0 bars/K) then can be used with the latent heat of fusion, 117.0 J/mole,[25] and the Clausius-Clapeyron equation to obtain $V_L^{tr} - V_s^{tr} = 2.73$ cm^3/mole. Our two extrapolated values of V_s^{tr} have a mean value of 23.477 (±0.05) cm^3/mole, so the molar volume of the fluid at the triple point can be calculated as V_L^{tr} = 26.21 (±0.05) cm^3/mole, in good agreement with the Goodwin and Roder[24] value of 26.176 (±0.05) cm^3/mole. Hence, we conclude that our data are internally consistent to within ±0.2%, and also they are consistent with other directly determined data to this same accuracy.

Kechin *et al.*[21] and Liebenberg *et al.*[9] have published molar volumes of the solid at melting for temperatures up to 164 K and pressures to 18.7 kbar. Their results are plotted in Fig. 10 in terms of deviations from the values calculated (V_{calc}) from Eq. (17), with the smallest molar volumes corresponding to approximately 10.9 cm^3. No overlap exists between our highest melting temperature (51.8 K) and the lowest temperature for the data of Liebenberg *et al.*[9] (75.0 K), so the reality of the change in slope and the validity of the high-temperature representation are open to question. The increase in dV_m/dT above 50 K could be due to relatively large increases in both γ and C_V with increasing temperature [see Eq. (19) and Sec. IV C].

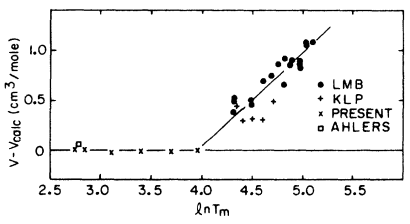

FIG. 10. Deviations from Eq. (17) for various determinations of the molar volume of solid p-H_2 along the melting line. Data are from Ref. 5 (Ahlers), Ref. 9 (LMB), and Ref. 21 (KLP, Kechin, Likhter, and Pavlyuchenko), as well as Table I (PRESENT).

C. Equation of state at high temperature and pressure

Driessen *et al.*[2] have generated an extrapolated high pressure EOS for solid p-H_2 which extends from $T = 0$ to the melting line and which is based on their adjusted version of the AS 4-K isotherm. This EOS is not in agreement with the direct melting line results of Liebenberg *et al.*[9] and Kechin *et al.*[21] The inconsistencies increase with increasing temperature and decreasing molar volume, and at 10.89 cm^3/mole the Driessen *et al.*[2] melting temperature is lower than the experimental value (163.9 K) by 14 K, and the melting pressure is approximately 9% smaller than the measured value (18.7 kbar). These differences are much larger than the uncertainties which are estimated.[2]

We have chosen to correlate the $P_0(V)$ relation of AS (Table X) and the melting line results[9,21] [$P_m(V, T_m)$] with the extrapolation of our heat capacity results to smaller volumes, instead of attempting to generate a "high temperature" EOS from our data by extrapolation. Equation (14) can be rewritten approximately as

$$P_m(V, T_m) = P_0(V) + \frac{\gamma}{V}\int_0^{T_m} C_V\, dT = P_0(V) + \frac{\gamma}{V}U_{th}, \tag{20}$$

where γ now becomes an effective Grüneisen parameter and U_{th} is calculated from heat capacities which are derived from Fig. 5 using the experimental T_m and $\Theta_0(V)$ as calculated from Eq. (7).

Such a calculation can be illustrated for a molar volume of 12.53 cm^3, for which Liebenberg *et al.*[9] give $T_m = 115.5$ K and $P_m = 9.779$ kbar, while Table X gives $P_0 = 8.152$ kbar, and Eq. (7) $\Theta_0 = 390.0$ K ($T_m/\Theta_0 = 0.296$). If the Θ/Θ_0 vs T/Θ_0 relation is assumed to be independent of volume at small molar volumes in the calculation of C_V (curve B in Fig. 5), Eq. (20) gives $\gamma = 2.25$. This postulate is equivalent to the assumption of a temperature-independent Grüneisen parameter, however, which should correspond to $\gamma_0 = 1.506$ from Eq. (8). This inconsistency can be resolved by assuming a family of curves in Fig. 5, each of which is similar to curve A and approaches a steep slope at the appropriate value of T_m/Θ_0. This postulate will permit a temperature-dependent γ with only small differences in U_{th} from those calculated using curve B.

The γ/γ_0 ratios calculated using Eq. (20) for the high temperature melting-line data[9,21] are plotted

as a function of T/Θ_0 in Fig. 11. The large scatter arises because the thermal term in Eq. (20) represents only 15% or so of the experimental melting pressures. The sharp increase in γ/γ_0 below our smallest molar volume ($T/\Theta_0 = 0.2$) is suggested in Fig. 7 and corresponds to the region where dV_m/dT is increasing rapidly (Fig. 10). We have to a first approximation assumed here that γ/γ_0 is a function only of T/Θ_0, and hence the ordinate in Fig. 11 is T/Θ_0, rather than T_m/Θ_0.

Equation (20) now can be used together with Table X, Eqs. (7) and (8), and the smoothed relations in Figs. 5 and 11 to calculate an EOS for solid hydrogen. This procedure is empirical, but since it is based on the Mie-Grüneisen EOS, it probably can be used for extrapolation to pressures and temperatures which correspond to the limit of the AS data, 9.8 cm^3/mole, or to approximately 30 kbar along the melting line.

D. The reduced EOS and its volume dependence

The reduced heat capacity relations (Fig. 5, Table VIII) resemble those for the rare-gas solids, with data for helium and neon showing a similar change in shape with decreasing volume.[27] The heavy rare-gas solids (neon, argon, krypton, xenon) have an appreciably less abrupt decrease in Θ/Θ_0 with increasing T/Θ_0 than does hydrogen, with the relations for helium only marginally different from those in Fig. 5 (see the summary in Fig. 11 of Ref. 27). The differences between the hcp solids helium and hydrogen and the fcc heavier rare-gas solids could be a crystal structure effect, since the helium results do not follow the trend with mass which is apparent for the fcc solids.

The systematic changes in shape with volume of the reduced relations in Fig. 5 (and of those for helium and neon[27]) correspond to a relative softening of the lattice vibrations with increasing temperature which becomes less marked for the smaller molar volumes. These effects could be due to larger mode Grüneisen parameters for high lattice frequencies than for small (mode γ's only volume dependent), or to explicit temperature effects on the lattice vibration spectrum (mode γ's contain an explicit temperature dependence as well as a volume dependence), or to both. The relative temperature dependence of the bulk modulus which is shown in Fig. 9 suggests that explicit temperature effects could exist for the lattice vibration spectrum, if the behavior of B_T is characteristic of that for the other elastic constants. These effects could arise as follows. The low-temperature EOS and hence the bulk modulus to a crude first approximation contain explicit contributions from both the static lattice and the zero point energy.[28,29] The solid is classical at high temperatures, however, so the zero point contribution must disappear for temperatures greater than Θ_0. These effects are most important for solid hydrogen for which the roughly 5 kbar zero point contribution to B_T can be estimated[28] to be approximately volume independent, and for which B_T varies from 1.7 kbar at 23.23 cm^3/mole to 12.5 kbar at 16.19 cm^3/mole. The static lattice contribution, which B_T should approach at high temperature, thus increases from −3.3 kbar (impossible in practice) to +7.5 kbar for these molar volumes. The behavior of B_T which is shown in Fig. 9 can be interpreted in terms of the initial stages (small T/Θ_0) of the decrease in the zero point contribution. A more appropriate (though less useful in practice) representation of Fig. 9 would have been in terms of T/Θ_0, from which it would have been evident that the relative decrease in B_T is greater for the larger molar volume ($T_m/\Theta_0 = 0.12$) than for the small ($T_m/\Theta_0 = 0.2$). By analogy, the other elastic constants should behave similarly, and the lattice vibration spectrum should show more relative softening with increasing temperature for large molar volumes than for small.

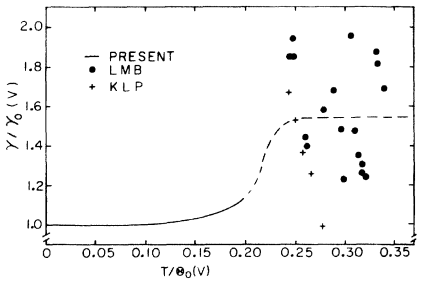

FIG. 11. Relative variation of the Grüneisen parameter with temperature as derived from the present results and measurements at higher temperatures and pressures along the melting line. The abbreviations are as in Fig. 10. See the text for details.

E. Phase transitions and premelting anomalies

Mills[30] has summarized various observations which suggest that phase transitions occur in p-H_2 at temperatures not far from the melting line and has proposed a phase diagram to correlate these. Silvera *et al.*[1] also survey earlier observations and report that they have not been able to confirm them. They suggest the possibility that the transitions may be shear induced and hence not observable in constant volume experiments such as theirs and ours. Holian[31] has calculated the phase diagram for an hcp-fcc phase transition in p-H_2, and predicts a relative volume change of 0.01% and a transition line slope dP/dT

= 150 bar/K near a 23-K triple point along the melting line.

A first-order transition will occur over a range of pressure and temperature in a constant-volume experiment. Any direct C_V or dP/dT measurement should show anomalously large measured values for data points which include this transition region. Holian's[31] predicted 23-K triple point occurs at a molar volume of approximately 20.5 cm^3, with a calculated latent heat of 0.7 J/mole, and (since $B_T \sim 3.6$ kbar) would be spread out over a region of a few mK or 0.4 bar. Our measured value of C_V is approximately 8 J/mole K under these conditions, with a typical temperature change of 0.5 K for a data point, so transition effects should have been observable. We do not obtain suspiciously high values for any of our data points for the four samples which include Holian's transition region. The possibility exists that, by chance, no data point included the transition region, although no anomalous warming rates were observed as the temperature drift was monitored between data points. While we cannot rule out the possibility that such a transition occurred in our experiments, we feel that it is highly unlikely.

We have commented elsewhere[8] about the possibility that the anomalous temperature-induced ortho-para conversion rate which we observe (see the dashed line in Fig. 8) could have been caused by a phase transition, and rule out this possibility. In general, our heat capacity data points can be represented by smooth relations to better than 1% at all temperatures. This includes data points for which the final temperature is closer than 0.5 K to the melting line. We find no evidence of a premelting anomaly for solid p-H_2.

F. Theoretical considerations

Silvera and Goldman[20] summarize various intermolecular potentials which have been used for calculations of the $T = 0$ properties of the hydrogen isotropes and propose a semiempirical pair potential which is quite successful in reproducing high-pressure solid state results for both hydrogen (Table X) and deuterium. The intermolecular potential of Etters *et al.*[32] which was the first to give good agreement with the experimental $P_0(V)$ relation at high pressures, has been used in a self-consistent phonon calculation[33] to obtain an improved $T = 0$ EOS for the hydrogen isotopes and also[34] to calculate temperature-dependent lattice properties for the hydrogen isotopes. This latter calculation gives only moderate agreement with the earlier $C_V(V, T)$ results of Ahlers[5] and hence with the present results. None of the calculations are particularly reliable at low pressures where the extremely small bulk modulus of solid hydrogen makes the prediction of V_0, for instance, difficult. Silvera and Goldman[18] assume the same form for the pair potential for both hydrogen and deuterium and determine three of the parameters by a fit to deuterium properties, including V_0. Their resulting pressure at Driessen *et al.*'s[2] value of V_0 (23.14 cm^3/mole), −15 bar, corresponds to $V_0 = 22.95$ cm^3/mole, and could result, as they state, either from differences in the pair potentials for the two isotopes, or from problems in the lattice dynamics. At present, the experimental thermodynamic data for p-H_2 at low pressure ($P_0 < 2$ kbar) appear to be more than adequate to test the predictions of existing theories. A recent calculation of volume-dependent elastic constants and Debye Θ's by Goldman,[35] for instance, gives Θ_0's which are too low by 10% or so.

V. CONCLUSIONS

The present experiment has resulted in a complete consistent determination of the thermodynamic properties of solid p-H_2 for molar volumes greater than 16.19 cm^3. These results confirm the less precise and extrapolated $P_0(V)$ relation of AS[3] and are in marginal agreement (barely within stated experimental uncertainties) with direct strain gauge measurements of the EOS over the same pressure range.[1,2] The thermodynamic properties can be correlated well using the Mie-Grüneisen model and a slightly temperature-dependent Grüneisen parameter. The volume dependence of the Grüneisen parameter has been determined directly [Eq. (8)] and is consistent with an approach to a constant value for very small volumes. An extrapolation to higher temperatures and pressures is consistent with direct measurements of thermodynamic properties along the melting line,[9,21] and a considerable (50%) increase in the Grüneisen parameter with increasing temperature. The temperature dependence at constant volume of the bulk modulus suggests that the temperature dependence of the Grüneisen parameter is associated with explicit variations with temperature of the lattice vibration spectrum. This is in agreement with observations by Silvera *et al.*[36] in Raman scattering measurements under pressure.

No direct comparisons with theoretical calculations are possible because of difficulties in calculations at large molar volumes. An extension of the present measurements to o-D_2 would be of considerable interest since, as Berkhart and Silvera[37] have stated, the apparent ratio of the Θ_0's

for H_2 and D_2 at V_0 for o-D_2 (19/95 cm^3/mole) is greater than 1.5 and is significantly different from the harmonic value of $\sqrt{2}$. A comparison of reduced plots for the two isotopes (Fig. 5) also would be of interest.

ACKNOWLEDGMENT

This work was supported by the U. S. Department of Energy, Contract No. W-7405-Eng-82, Division of Basic Energy Sciences, AK-01-02-02-2.

*Present address: Department of Physics, University of Delaware, Newark, Delaware 19711.

[1]I. F. Silvera, A. Driessen, and J. A. de Waal, Phys. Lett. A 68, 207 (1978).
[2]A. Driessen, J. A. de Waal, and I. F. Silvera, J. Low Temp. Phys. 34, 255 (1979).
[3]M. S. Anderson and C. A. Swenson, Phys. Rev. B 10, 5184 (1974).
[4]J. K. Krause, USDOE Report No. IS-T-844-1978 (unpublished). (Available from the National Technical Information Service, U. S. Department of Commerce, Springfield, VA 22151.)
[5]G. Ahlers, J. Chem. Phys. 41, 86 (1964).
[6]R. Q. Fugate and C. A. Swenson, J. Low Temp. Phys. 10, 317 (1973).
[7]R. J. Roberts and J. G. Daunt, J. Low Temp. Phys. 6, 97 (1972).
[8]J. K. Krause and C. A. Swenson, Solid State Commun. 31, 835 (1979).
[9]D. H. Liebenberg, R. L. Mills, and J. C. Bronson, Phys. Rev. B 18, 4526 (1978).
[10]G. Ahlers, Ph.D. thesis, University of California at Berkeley, 1963 (unpublished).
[11]R. D. Goodwin, Cryogenics 2, 353 (1962).
[12]J. K. Krause and C. A. Swenson, Cryogenics 16, 413 (1976).
[13]R. Schweitzer, S. Washburn, and H. Meyer, Phys. Rev. Lett. 40, 1035 (1978).
[14]J. F. Jarvis, H. Meyer, and D. Ramm, Phys. Rev. 178, 1461 (1969).
[15]W. R. Gardner, J. K. Hoffer, and N. E. Phillips, Phys. Rev. A 7, 1029 (1973). This paper gives a reanalysis of previous data for helium and a different $\gamma(v)$ relationship from that of Ahlers, Phys. Rev. A 2, 1505 (1970).
[16]V. A. Popov, V. B. Kokshenev, V. G. Manzhelli, M. A. Strzhemechney, and V. I. Voitovich, J. Low Temp. Phys. 26, 979 (1977).
[17]M. Nielsen, Phys. Rev. B 7, 1626 (1973).
[18]P. J. Thomas, S. C. Rand, and B. P. Stoicheff, Can. J. Phys. 56, 1494 (1978).
[19]B. A. Younglove, J. Chem. Phys. 48, 4181 (1968).
[20]I. F. Silvera and V. A. Goldman, J. Chem. Phys. 69, 4209 (1978).
[21]V. V. Kechin, A. I. Likhter, Yu M. Pavlyuchenko, L. Z. Ponsovskii, and A. N. Utyuzh, Sov. Phys. JETP 45, 182 (1977).
[22]R. F. Dwyer, G. A. Cook, B. M. Shields, O. E. Berwaldt, and H. E. Nevins, J. Chem. Phys. 43, 801 (1965).
[23]R. F. Dwyer, G. A. Cook, B. M. Shields, and D. H. Stellrecht, J. Chem. Phys. 42, 3809 (1965).
[24]R. D. Goodwin and H. M. Roder, Cryogenics 3, 12 (1963).
[25]H. M. Roder, G. E. Childs, R. D. McCarty, and P. E. Angerhofer, Natl. Bur. Stand. (U.S.) Tech. Note 641 (1973). Available as SD Catalog No. C13.46:641,1973, Superintendent of Documents, U. S. GPO, Washington, D. C.
[26]E. R. Grilly (private communication).
[27]C. A. Swenson, in *Rare Gas Solids* (Academic, London, 1977), Vol. 2, Chap. 13.
[28]C. A. Swenson, J. Phys. Chem. Solids 29, 1337 (1968).
[29]M. S. Anderson and C. A. Swenson, J. Phys. Chem. Solids 36, 145 (1975).
[30]R. L. Mills, J. Low Temp. Phys. 31, 423 (1978).
[31]Brad Lee Holian, Phys. Rev. B 18, 4780 (1978).
[32]R. D. Etters, R. Danilowicz, and W. England, Phys. Rev. A 12, 2199 (1975).
[33]A. B. Anderson, J. C. Raich, and R. D. Etters, Phys. Rev. B 14, 814 (1976).
[34]A. B. Anderson, J. C. Raich, and L. B. Kanney, Phys. Rev. B 15, 5804 (1977).
[35]V. V. Goldman, J. Low Temp. Phys. 36, 521 (1979).
[36]I. F. Silvera, P. J. Berkhout, and L. M. van Aernsbergen, J. Low Temp. Phys. 35, 611 (1979).
[37]P. J. Berkhout and I. F. Silvera, J. Low Temp. Phys. 36, 231 (1979).